

Poly(ADP-Ribose) Polymerase-1 (PARP-1) Inhibitors Based on a Tetrahydro-1(2H)-isoquinolinone Scaffold: Synthesis, Biological Evaluation and X-ray Crystal Structure

Stefan Peukert,*¹ Uwe Schwahn, Stefan Güssregen, Herman Schreuder, Armin Hofmeister

Aventis Pharma Deutschland GmbH, a company of the sanofi-aventis group, TD Cardiovascular, TD Thrombosis and Angiogenesis and Chemical Sciences, 65926 Frankfurt, Germany

Fax +49(69)331399; E-mail: armin.hofmeister@sanofi-aventis.com

Received 23 December 2004

Dedicated to Professor Bernd Giese on the occasion of his 65th birthday

Abstract: The synthesis, activity and physical properties of two series of novel potent tetrahydro-1(2H)-isoquinolinone based PARP-1 inhibitors are described. The new structural classes with a non-planar ring system interact specifically with the PARP-1 protein at the nicotinamide-binding site.

Key words: medicinal chemistry, PARP inhibitors, structure-activity relationship, isoquinolinones, crystal structure

Introduction

Poly(ADP-ribose) polymerase-1 (PARP-1, EC 2.4.2.30), the most prominent member of the PARP family, is a DNA-binding protein activated by nicks in DNA occurring during inflammation, ischemia, neurodegeneration or cancer therapy.² Activated PARP-1 consumes NAD⁺ that is cleaved into nicotinamide and ADP-ribose and polymerizes the latter onto nuclear acceptor proteins. This process is pivotal for the maintenance of genomic stability. When over-activated, however, PARP-1 can cause extensive polymerization of ADP-ribose, leading to the depletion of NAD⁺ and, subsequently, a decrease in the level of intracellular ATP. This depletion of ATP can culminate in cell dysfunction and cell death through a necrotic pathway.³ Studies done with PARP-1 deficient mice demonstrated that a lack of PARP-1 renders them resistant to cerebral ischaemia.⁴ This observation was supplemented by recent work with potent inhibitors demonstrating the beneficial effects of PARP inhibition in animal models of stroke, heart ischemia and cancer.⁵ Therefore, PARP-1 is regarded as a promising target for the development of drugs useful in various forms of inflammation, ischemia-reperfusion injury and as an adjunct in cancer therapy.

The overwhelming majority of known PARP inhibitors bind to the nicotinamide-binding site, where they act as competitive inhibitors to NAD⁺. As depicted in Figure 1, the carboxamide moiety of nicotinamide forms three hydrogen bonds with the catalytic domain of PARP-1; one to the hydroxyl group of Ser904 and two to the amide backbone of Gly863.⁶ This binding mode requires the carbox-

amide carbonyl group to be in the *anti*-conformation **1a** that is in equilibrium with the *syn*-conformation **1b**. The first PARP inhibitors identified, such as 3-aminobenzamide (**2**), are close structural analogues to the nicotinamide moiety of NAD⁺.⁷ However, this compound lacks good potency, which can be attributed to the conformational flexibility of the carboxamide carbonyl group. Hence, restricting this carbamoyl moiety to the *anti*-conformation by formation of an adjacent ring led to new generations of compounds as shown in the isoquinolinone **3**, 5[*H*]phenanthridin-6-one **4** or dihydrocyclopenta[*lmn*]phenanthridin-5-one **5** series which were more potent by several orders of magnitude^{7,8} (Figure 1).

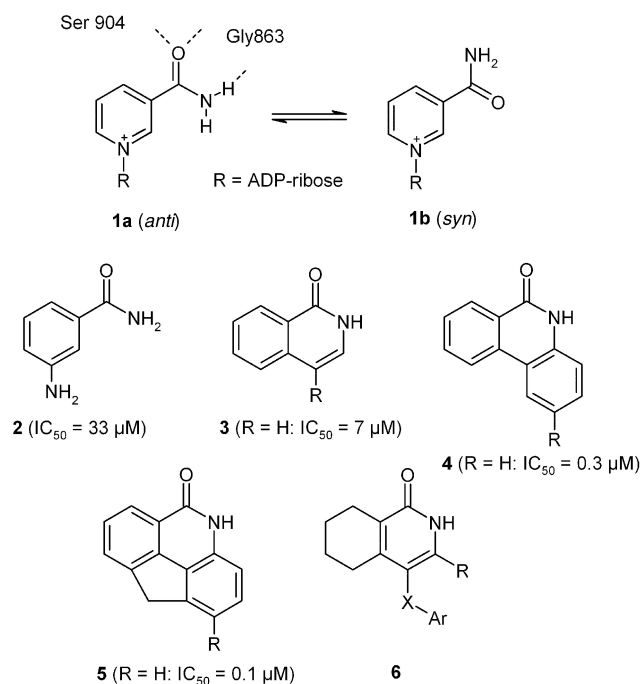


Figure 1 Structural requirements for PARP inhibition and classes of PARP-1 inhibitors

Despite this improvement in potency, clinical development is still slow which might be attributed to safety issues. As mentioned above, most PARP inhibitors have extended planar structures that can have DNA-intercalating properties.⁹ Therefore, inhibitors with less planar

SYNTHESIS 2005, No. 9, pp 1550–1554

Advanced online publication: 19.04.2005

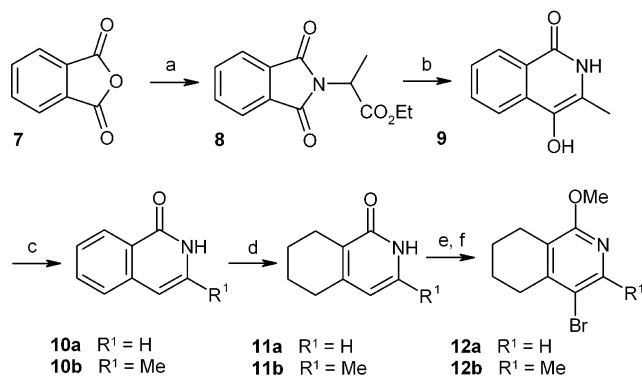
DOI: 10.1055/s-2005-865324; Art ID: C05404SS

© Georg Thieme Verlag Stuttgart · New York

structures, which should be devoid of this unwanted property are desirable. Herein, we describe substituted 5,6,7,8-tetrahydro-1(2*H*)-isoquinolinones **6** as PARP-1 inhibitors. This class of compounds was designed to overcome the planar ring system found in known PARP-1 inhibitors albeit maintaining their good potency.

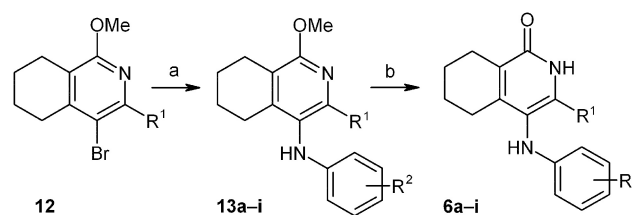
Chemistry

The synthesis of the key building blocks **12** is outlined in Scheme 1. The preparation of the methyl-substituted compound **12b** started with phthalic anhydride (**7**), which was heated with ethyl 2-aminopropionate to yield the phthalimidopropionate **8** in 89% yield. Phthalimido ester rearrangement in the presence of sodium methoxide afforded the hydroxyisoquinolinone **9** which was reduced to isoquinolinone **10b** in hydroiodic acid in the presence of red phosphorus in moderate yield after extended periods of time.¹⁰ Hydrogenation of **10b** in acetic acid at 5 bar in the presence of platinum resulted in 5,6,7,8-tetrahydroisoquinolinone **11b** which could be easily isolated by recrystallization from methanol in 83% yield. In the case of the commercially available isocarbostyryl (**10a**) the hydrogenation occurred less selectively and provided next to the desired **11a** (60% yield) some 3,4-dihydro-2*H*-isoquinolin-1-one, which could be removed by recrystallization from water. Both compounds were excellent substrates for bromination in 4-position: **11a** was brominated with bromine in chloroform whereas **11b** reacted best with *N*-bromosuccinimide in methanol. The intermediates were subsequently *O*-methylated with methyl iodide in the presence of silver carbonate to afford **12a** and **12b**, respectively. The transformation into the annulated methoxy-pyridines proved necessary, as palladium-catalyzed reactions did not proceed with the brominated 5,6,7,8-tetrahydroisoquinolinones. Compounds **6** substituted with anilines could be prepared in moderate yields by Hartwig–Buchwald amination from bromides **12** employing micro-



Scheme 1 Reagents and conditions: a) ethyl 2-aminopropionate, 120 °C, 89%; b) NaOMe, MeOH, reflux, 63%; c) red P, 55% HI, 160 °C, 46%; d) PtO₂, H₂ (3–5 bar), AcOH, 60–83%; e) **12a**: Br₂, CHCl₃, 5 °C, 96%; **12b**: NBS, MeOH, 0 °C, 84%; f) MeI, Ag₂CO₃, CHCl₃, 50 °C, 83–84%

wave conditions as shown in Scheme 2. Deprotection of the pyridone functionality with chlorotrimethylsilane and potassium iodide furnished cleanly the analogues **6a–i**.



Scheme 2 Reagents and conditions: a) aniline, *t*-BuONa, toluene, Pd₂dba₃, *t*-Bu₂P-biphenyl, 150 °C, microwave; b) TMSCl, KI, MeCN, 60 °C

Synthesis of the furyl substituted compounds **6j–u** originated from bromides **12** as well. Suzuki coupling using the Fu conditions furnished aldehydes **14**.¹¹ The requisite 5-formylfuran-2-boronic acid is either commercially available or can be prepared by an excellent protocol from the patent literature.¹² Deprotection with chlorotrimethylsilane and potassium iodide yielded aldehydes **15**, which were subjected to reductive amination employing polymer-bound triacetoxyborohydride in THF. The use of the polymer-bound reducing agent facilitated the work-up procedure and allowed better recovery of the water-soluble analogues **6j–s**. Compound **6t** (R¹, R³ and R⁴ = H) was prepared by reductive amination of **15a** with sodium borohydride in the presence of a large excess of ammonium acetate. This compound served as starting material for the preparation of analogue **6u** by acylation with nicotinoyl chloride.

Results and Discussion

All compounds were fully characterized by ¹H NMR spectroscopy, high resolution MS and HPLC and were tested as inhibitors for human PARP-1 (see experimental section). Solubility was determined in phosphate buffered saline at pH 7.4 (24 h equilibrium). Two series of potent 4-substituted tetrahydro-1(2*H*)-isoquinolinones were identified, namely the aniline substituted compounds (Table 1, **6a–i**) and the furyl substituted compounds (Table 2, **6j–u**) (Scheme 3). Table 1 shows the structure–activity relationship (SAR) for a series of simple substituents R¹ and R². Compounds with a methyl group at the R¹ position (**6a,c**) proved to be 3–7 fold more potent than the corresponding analogues derivatives with hydrogen at this position (**6g,h**). A possible explanation for this could be that the methyl group at R¹ position has a favorable entropical effect by restricting the conformations of the aniline moiety. The most active compounds **6a** and **b** both have a R² substituent with a carbonyl functionality indicating a strong and specific interaction with the enzyme-binding site. This hypothesis was later verified by an inhibitor/enzyme crystal structure with **6a** (see next section). Compound **6d** with the inverted amide functionality

Table 1 Structure–Activity Relationship for Compounds **6a–i** Bearing an Aniline Substituent

	R ¹	R ²	IC ₅₀ (μM)
6a	Me	COMe	0.09
6b	Me	CONMe ₂	0.08
6c	Me	SO ₂ Me	0.30
6d	Me	NHCOMe	0.14
6e	Me	OCF ₃	1.21
6f	Me	CH ₂ OH	0.61
6g	H	COMe	0.69
6h	H	SO ₂ Me	0.80
6i	H		1.43

presumably can still develop the same interaction albeit with slightly decreased strength. The same seems to be true for compound **6c** with a methanesulfonyl substituent at this position. Compounds that lack a hydrogen acceptor at this position (e.g. **6e**) showed diminished potency. Compound **6f** regained some of the potency as the oxygen of the hydroxylmethyl group might serve as acceptor instead of a carbonyl oxygen. Attempts to further increase the potency by restricting the rotational freedom of the carbonyl group by incorporating it into a ring (**6i** vs **6g**) were not successful, indicating the sensitivity of the interaction between this functionality and the binding site. Compound **6a** was further profiled and showed next to the IC₅₀ value of 90 nM a low inhibitory constant ($K_i = 54$ nM) and EC₅₀ value in the cell-protection assay of 0.2 μM.

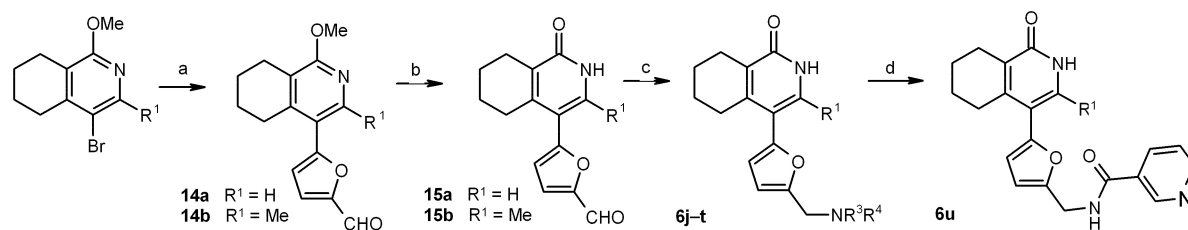
In the furyl series the difference in potency between compounds **6j–l** with a methyl substituent at the R¹ position

Table 2 Structure–Activity Relationship for Compounds **6j–u** Bearing a Furyl Substituent

	R ¹	R ³ /R ⁴	IC ₅₀ (μM)	Sol. (mg/mL) ^a
6j	Me	-(CH ₂) ₄ -	0.30	2.40
6k	Me	H, Bu	0.24	n.d.
6l	Me	H, 1-methylpyrazol-4-ylmethyl	0.33	3.40
6m	H	-(CH ₂) ₄ -	0.11	1.97
6n	H	H, Bu	0.25	0.82
6o	H	H, 1-methylpyrazol-4-ylmethyl	0.18	n.d.
6p	H	H, CH ₂ Ph	0.15	n.d.
6q	H	1-methylimidazol-2-ylmethyl, CH ₂ Ph	2.76	n.d.
6r	H	H, (CH ₂) ₂ NMe ₂	0.46	1.41
6s	H	H, pyridin-3-ylmethyl	0.99	12.18
6u	H	H, nicotinoyl	0.79	n.d.

^a n.d.: Not determined.

and the corresponding unsubstituted compounds **6m–o** is small with a slight preference for the unsubstituted compounds. The SAR regarding R³/R⁴ is somewhat flat as shown in examples **6m–p** and **r**. Secondary and primary aliphatic, heteroaromatic, aromatic and basic functionalized side chains were all tolerated, indicating that this part of the molecule is not involved in specific interactions with the binding site. As seen from the X-ray structure of compound **6j** (see next section), the main interaction at this portion of the molecule is between the positively charged nitrogen and a conserved water molecule in the binding site. However, steric bulk is of importance as demonstrated with compound **6q**. This tertiary amine with



Scheme 3 Reagents and conditions: a) 5-formylfuran-2-boronic acid, Pd₂dba₃, KI, (*t*-Bu)₃PHBF₄, THF, 60 °C, 79–100%; b) TMSCl, KI, MeCN, 60 °C, 27–55%; c) macroporous BH(OAc)₃ or NaCNBH₃, THF, amine; d) nicotinoyl chloride, Et₃N, CH₂Cl₂

two larger substituents R³/R⁴ showed clearly diminished potency compared to smaller secondary amines **6o** or **p**. Interestingly, pyridyl substituted compounds **6s** and **u** exhibited comparable activity although **6u** with an amide functionality cannot form the interaction described for the amine functionality. Modeling studies suggest that in this case the pyridyl nitrogen of **6u** forms a weak hydrogen bond to the Arg878 main chain nitrogen that compensates for the loss of the interaction of the amine functionality mentioned above.

Compounds **6j–u** typically showed excellent solubilities in aqueous solution at pH 7.4 which make them readily suitable for intravenous applications. Moreover, compound **6j** exhibited an inhibitory constant of 15 nM and an EC₅₀ value of 0.33 μM in the cell-protection assay compared to the free enzyme IC₅₀ value of 0.30 μM, which demonstrates its good cell permeability.

Structural Data

The observed SAR can be explained with the aid of two crystal structures of the active fragment of chicken PARP-1 in the presence of the aniline substituted inhibitor **6a** and the furan-substituted inhibitor **6j** (Figure 2a,b).¹³

Both inhibitors are bound in the donor NAD⁺ site, as identified by Ruf et al.¹⁴ The N-terminal domain in our structures is slightly rotated with respect to the PARP structures available in the protein data bank (PDB), leading to an average root-mean-square displacement of about 1.5 Å for this domain. At present it is not possible to determine whether it is due to our particular crystallization conditions (r.t. vs. 4 °C), or whether the inhibitors induce this conformational change.

The binding mode of the tetrahydroisoquinolinone ring system is the same for both inhibitors. The pyridone ring is stacked between the aromatic side chain of Tyr907, the main-chain atoms of Tyr896 and Phe897 and the side

chain of His862. The N of the pyridone ring interacts with the carbonyl oxygen of Gly863, while the carbonyl oxygen of the pyridone interacts with the main chain N of the same Gly863. In addition, this carbonyl O makes also a hydrogen bond with the hydroxyl side chain of Ser904. The annulated cyclohexyl ring forms optimal van der Waals contacts with the protein and occupies the same space as the benzene ring in other bicyclic lactam inhibitors. Modeling studies suggest that this is the position of the aromatic part of the nicotinamide ring of the natural substrate NAD⁺.⁶

The 3-acetylphenyl group of **6a** is oriented almost perpendicular to the pyridone ring. The carbonyl oxygen displaces a water molecule and interacts with the main-chain nitrogen of Tyr896, which can explain the high potency of compounds **6a** and **b**.

The furan ring of **6j** is also almost perpendicular to the pyridone ring at about the same position as the 3-acetylphenyl group of **6a**. However, the pyrrolidine ring is at a position about 90° away from the position of the acetyl substituent of **6a**. The pyrrolidine nitrogen is involved in a strong hydrogen bond to a bound water molecule, which is held in place by hydrogen bonds to the side chains of Gln763 and Glu766 and another water molecule in the network of water molecules in the PARP active site. We did not observe any further specific interactions between either the furan ring or the pyrrolidine ring and the protein.

In conclusion, we have discovered and optimized substituted tetrahydro-1(2*H*)-isoquinolinones as a new class of PARP-1 inhibitors. Apart from high potency, compounds with excellent solubility could be identified and their binding conformation has been evaluated with X-ray crystal structures of the ligands and the PARP-1 protein. The use of these non-planar inhibitors which could be advantageous in terms of non-mechanism based side effects is currently studied in vivo.

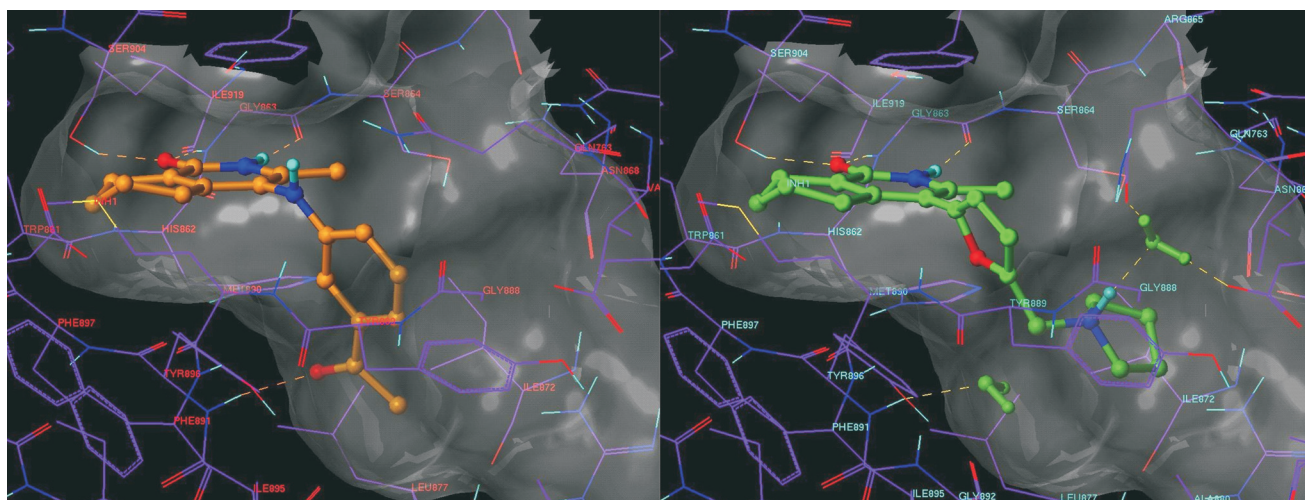


Figure 2a (left): Crystal structure of compound **6a** and cPARP-1 protein;

Figure 2b (right): Crystal structure of compound **6j** and cPARP-1 protein

PARP Enzyme Inhibition Assay

The inhibitory potency of substances was measured in an enzymatic assay using recombinant human PARP-1 protein. In a 50 μ L total reaction volume, 2 μ g/mL enzyme were incubated with different concentrations of test substance in a buffer containing Tris (50 mM), MgCl₂ (5 mM), dithiothreitol (1 mM), NAD (200 μ M), tritiated NAD (0.1 mCi/mL), sheared DNA (0.1 mg/mL) and histone (0.1 mg/mL) at pH 8.0. After 1 h incubation at r.t., the reaction was stopped by adding aq 20% trichloroacetic acid (150 μ L) and incubated on ice for 10 min. Protein precipitates were collected on glass fiber filters, washed three times with aq 20% trichloroacetic acid and incorporated radioactive poly(ADP-ribose) polymer was measured in a Wallac Trilux Microbeta by liquid scintillation counting. IC₅₀ values were determined as the substance concentration at which precipitable radioactivity reached 50% of the value attainable by incubation of the reaction mixture with solvent only. Inhibitory constants (K_i) of the test substances were determined with the same enzyme reaction as described above, only that different concentrations of the substrate NAD were used and the incubation time was reduced to 10 min. K_i values were determined by linear regression assuming a purely competitive mechanism of inhibition.

ATP Consumption Assay in Cardiomyoblasts

The protective potency of the substances was measured in a cellular model of cytotoxic injury. Rat cardiomyoblasts (H9c2) were seeded at 40,000 cells per well in a 96-well plate and incubated overnight in RPMI1640, 10% fetal calf serum. Then cells were pretreated for 15 min with different concentrations of the test substance and after adding H₂O₂ (300 μ mol) the cells were lysed for 1 h and ATP content determined by luciferase reaction. The half-maximal effective concentration (EC₅₀) of the substances was determined as the concentration at which the ATP content of injured cells reached 50% of the level that could maximally be attained by the same compound at higher substance concentrations.

Acknowledgment

We wish to thank Horst Plankenhorn and Michael Schnierer for their technical assistance in the synthesis of the compounds and also Antje Schlüter for her assistance in the biological evaluation of the compounds. We also thank Alexander Liesum, Volker Brachvogel and Petra Lönze for excellent technical assistance with the crystallization, data collection and refinement of the structures.

References

- (1) New address: S. Peukert, Novartis Institutes for Biomedical Research, 250 Massachusetts Avenue, Cambridge, MA 02139, USA; E-Mail: stefan.peukert@novartis.com.
- (2) Review: Smith, S. *Trends Biochem. Sci.* **2001**, *26*, 174.
- (3) Review: Virag, L.; Szabo, C. *Pharmacol. Rev.* **2002**, *45*, 73.
- (4) Eliasson, M. J. L.; Sampei, K.; Mandir, A. S.; Hurn, P. D.; Traystman, R. J.; Bao, J.; Pieper, A.; Wang, Z.-Q.; Dawson, T. M.; Snyder, S. H.; Dawson, V. L. *Nat. Med.* **1997**, *3*, 1089.
- (5) (a) Komjati, K.; Mabley, J. G.; Virag, L.; Southan, G. J.; Salzman, A. L.; Szabo, C. *Int. J. Mol. Med.* **2004**, *273*, 373. (b) Ferraris, D.; Ko, Y. S.; Pahutski, T. *J. Med. Chem.* **2003**, *46*, 3138. (c) Calabrese, C. R.; Almasy, R.; Barton, S.; Batey, M. A.; Calvert, A. H.; Canan-Koch, S.; Durkacz, B. M.; Hostomsky, Z.; Kumpf, R. A.; Kyle, S.; Li, J.; Maegley, K.; Newell, D. R.; Notarianni, E.; Stratford, I. J.; Skalitzyk, D.; Thomas, H. D.; Wang, L.-Z.; Webber, S. E.; Williams, K. J.; Curtin, N. J. *J. Natl. Cancer Inst.* **2004**, *96*, 56.
- (6) Ruf, A.; De Murcia, G.; Schulz, G. E. *Biochemistry* **1998**, *37*, 3893.
- (7) Banasik, M.; Komura, H.; Shimoyama, M.; Ueda, K. *J. Biol. Chem.* **1992**, *267*, 1569.
- (8) Li, J.-H.; Tays, K. L.; Zhang, L. Guildford Pharmaceuticals WO 9911624, **1999**; *Chem. Abstr.* **1999**, *130*, 218328.
- (9) Peukert, S.; Schwahn, U. *Exp. Opin. Ther. Pat.* **2004**, *14*, 1531.
- (10) Falk, H.; Suste, A. *Monatsh. Chem.* **1994**, *125*, 325.
- (11) Netherton, M. R.; Fu, G. C. *Org. Lett.* **2001**, *3*, 4295.
- (12) Meudt, A. Clariant GmbH, WO 03033503, **2003**; *Chem. Abstr.* **2003**, *138*, 321392.
- (13) The catalytic fragment of chicken PARP-1 was obtained from Prof. DeMurcia of the Ecole Supérieure de Biotechnologie de Strasbourg. Native PARP-1 was crystallized at pH 8.5 with 18% PEG 4000 and 8% *i*-PrOH as precipitant, following the protocol of Jung et al.: Jung, S.; Miranda, E. A.; De Murcia, J. M.; Niedergang, C.; Delarue, M.; Schulz, G. E.; DeMurcia, G. M. *J. Mol. Biol.* **1994**, *244*, 114. Inhibitor complexes were obtained by soaking native crystals with the appropriate inhibitors. The space group and cell dimensions of the crystals obtained were the same as in the published crystal structures. We obtained well diffracting crystals, diffracting to 2.2 and 2.1 Å resolutions, respectively. We did not observe any major differences between our PARP structures and the PARP structures present in the PDB.
- (14) Ruf, A.; De Murcia, J. M.; De Murcia, G. M.; Schulz, G. E. *Proc. Natl. Acad. Sci. U.S.A.* **1996**, *93*, 7481.